Proceedings of the Korean Nuclear Society Spring Meeting
Cheju, Korea, May 2001

A Gas Avalanche Chamber Operated with a Secondary Electron Emitter in Radiation Detection

Il Jin Park, Nam Ho Lee, Hyun Kyu Jung, Seung Ho Kim
J. Kadyk*, and V. Perez-Mendez*

Korea Atomic Energy Research Institute
Yusong, Taejon, Korea 305-600

*Lawrence Berkeley National Lab.
Berkeley, CA94720, USA

Abstract

A columnar CsI secondary electron emitter has been coupled to a conventional microstrip chamber. The characteristics of a columnar CsI with gas multiplication was investigated by using beta rays from a ^{90}Sr source. This layer is intended for use as the primary electron source in any gas avalanche microdetector to avoid severe performance loss by the oblique angle of the incident charged particle. It was initially thought that the columnar structure might provide a larger detection efficiency than a planar CsI layer, because of the many surface crossings of incident particle for the columnar geometry. The efficiency measurement of a columnar CsI layer was performed in a thin parallel-plane structure, which has a 50-500 μm gas gap between a columnar CsI cathode and metal anode. We discuss the secondary emission and electric fields in the columnar structure, and explain why, based upon field simulation and experimental results, this approach does not succeed in this case. New ideas are presented for driftless gas avalanche detectors insensitive to the angle of incidence.

I. Introduction

Currently there is a great deal of activity in the development of microstructure gas detectors with good spatial resolution and high rate capability. In spite of many attractive features, these detectors perform poorly when the particle is not incident nearly perpendicular to the plane of the detector. The spread of primary electrons along the track in the drift region degrades the detection efficiency as well as the spatial and timing resolutions of the detectors.

Recently, there has been an increasing interest in combining avalanche amplification and secondary electron emission (SEE) for detection of radiation [1,2]. When the charged particles hit the surface of a solid, the latter may emit secondary electrons of low energy (< 50 eV). The escape mechanism for these electrons is similar to the emission of photoelectrons in the photoelectric effect. This is the reason that good photocathode materials are also usually good secondary emitters.

The emission mechanisms have three distinct parts. The first is the production of a cloud of electrons in the material; the second part consists of migration of these electrons to the surface, and finally there is emission of secondary electrons from the surface. The probability of secondary electron emission depends strongly on the rate of energy loss dE/dx, of the incident particle.

The use of a secondary electron emitter as the primary source of electrons in a gas avalanche detector has been tested [1,3]. With this approach using a planer layer, the time resolution was improved by more than one order of magnitude, compared with a conventional microstrip gas chamber (MSGC), and no angular dependence of the efficiency was observed [3]. However, the efficiency was low.

For most materials, the SEE efficiency is only a few percent. On the other hand, alkali-halide porous materials such as CsI and KCl have a much larger emission efficiency [4]. The efficiency of a single porous CsI layer has been measured to be 55 % by Chianelli et al. [5]. This result suggest that efficiency of a secondary emitter can be increased by having many surface crossings of each incident particle.

A columnar CsI(Tl) layer has been extensively used for X-ray medical imaging [6] because of the advantage of light channeling. The columnar structure allows many surface crossings by an incident particle, Therefore, we initially thought that a columnar structure of pure CsI might improve the SEE efficiency.

As we shall see, subsequent tests and simulations show that secondary emission is limited to only the top surface of the CsI layer. Characteristics such as a efficiency and pulse height distribution for electrons from ^{90}Sr source were measured using P10 (Ar 90 % + CH_4 10 %) gas.

II. Structure

Figure 1 shows a scanning electron microscope (SEM) photograph of a columnar CsI layer. The diameter of the CsI columns was measured to be about 5 μm and the spacing between the column walls was to be about 3-5 μm.

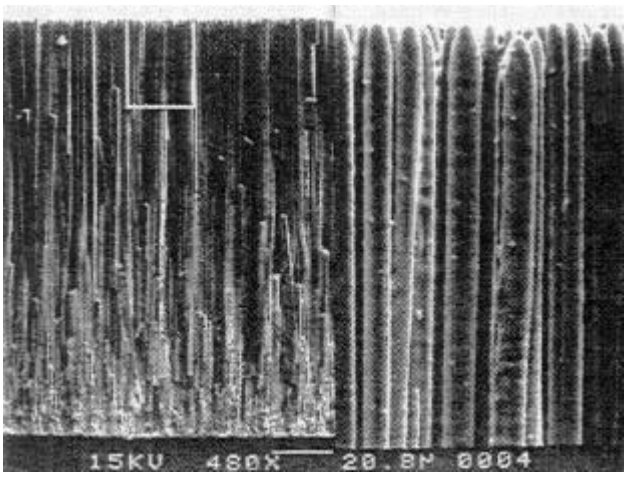

Figure 1: Scanning Electron Microscope (SEM) photograph of a columnar CsI layer of 100 μm thickness.

The column diameter and the gap between columns depend on parameters during the manufacture, such as argon pressure in the evaporation chamber, substrate temperature and angle between substrate and evaporation boat, etc.

In our case, the substrates are placed in rotating holder, which has a cooling system to maintain the substrate at 120 °C. The angle of deposition 45° was relative to the holder. The evaporation chamber was initially pumped down to 10^{-6} torr and filled with argon to a pressure of 5 mtorr.

III. A Columnar CsI Layer as a Drift Plane of MSGC

A. Pulse height enhancement

To investigate the characteristics of the columnar CsI layer, we initially mounted the CsI layer on a drift plane of microstrip gas chamber (MSGC). Figure 2 shows a schematic diagram of a MSGC coupled with a columnar CsI layer. This method uses the same fundamental idea as in previous approaches: an incident charged particle provides the source of primary electrons by the SEE process, predominantly from a very small region, or ' point' on the drift plane. For an inclined track the concentration of electron production allows primary electrons to be focused on anode, which lead directly to the improvements in spatial resolution and the time resolution.

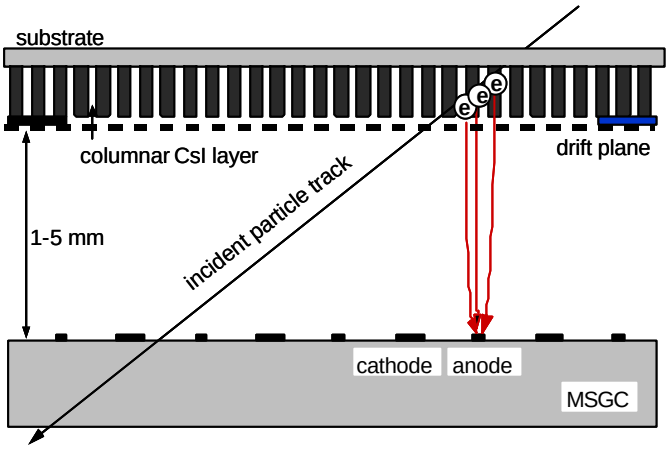

Figure 2: A conventional MSGC coupled with a 300 μm columnar CsI secondary electron emitter added to the drift plane.

A collimated ^{90}Sr beta ray source was used for the measuremets. The chamber was filled with Ar/Ethane (50/50) gas mixtures. A 125 μm thickness kapton pieces were placed between the columnar layer and the drift plane as a spacer. Figure 3 (a) shows pulse-height spectra of the ^{90}Sr beta source, for V_{csi}=0 and –1600 V, where V_{csi} is the voltage applied across the CsI layer. Figure 3(b) shows measurements of relative signal enhancement as a function of applied voltage across the CsI layer. The electron multiplication factor due to the CsI layer is defined as the ratio of signal-pulse amplitude produced when V_{csi} is turned on to that produced when V_{csi} is turned off. As can be seen, a large amount of electron amplification occurs within the CsI layer when it is activated, greatly enhancing the signal-pulse amplitude over that coming from the ionization in the gas drift region alone. This remarkable enhancement is due to combining primary electrons initialized from the CsI surface with a gas avalanche in the gas gap between the columnar layer and the drift plane.

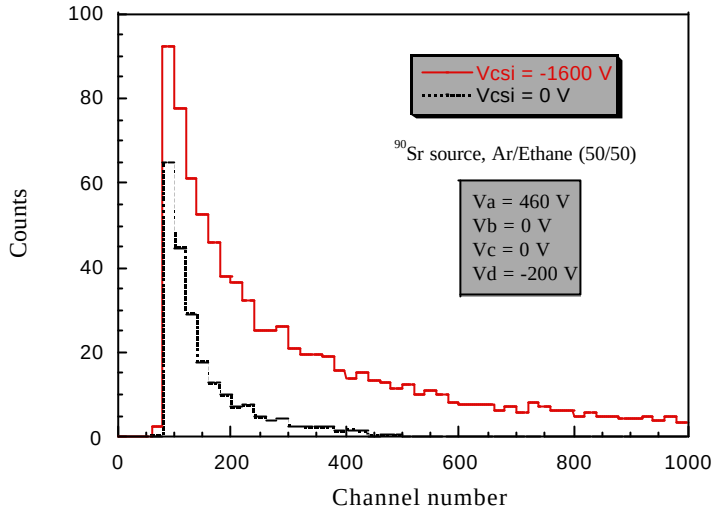

(a)

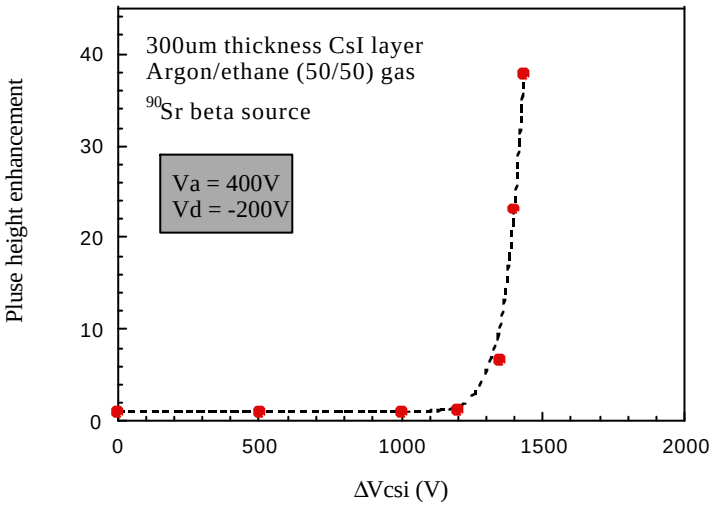

(b)

Figure 3: Pulse-height spectra of the ^{90}Sr beta source, using a conventional MSGC coupled with a columnar CsI layer, for V_{csi} = 0 and -1600 V. Here V_{csi}, V_a, V_c, and V_d are voltage applied to the CsI layer, anode strips, cathode strips, and drift plane, respectively.

B. Timing resolution

In large number of applications, information of precise arrival time of a quantum of radiation in the detector is of particular interest. In conventional MSCG, the timing resolution has been measured about 20 ns rms. The time resolution of a gas avalanche detector significantly depend on the length of drift gap, for the primary electrons are distributed along the incidence particle track in the gas gap. However, the use of a secondary electron emitter in a gas avalanche detector can provide a good timing resolution due to the "point-like" source of primary electrons. The timing measurement system is shown in figure 4(a). P10 gas, Ar/Methane (90/10), and ^{90}Sr source was used in this measurement. This experiment performed at reduced gas pressure which was 30 torr, in order to eliminate the possible primary source in the gas gap. In this system, timing filter amplifier (TFA) were used for fast shaping time. The signal from each TFA were connected to constant fraction discriminator (CFD) for accurate timing and the CFD signals were used as the start and stop signals

in a timid to amplitude converter. The result is shown in figure 4(b). As expected, the CsI layer improves timing of the coupled MSGC by a large factor. The timing resolution for MSGC coupled to a columnar CsI was determined to 5.5 ns rms at reduced gas pressure, 30 torr.

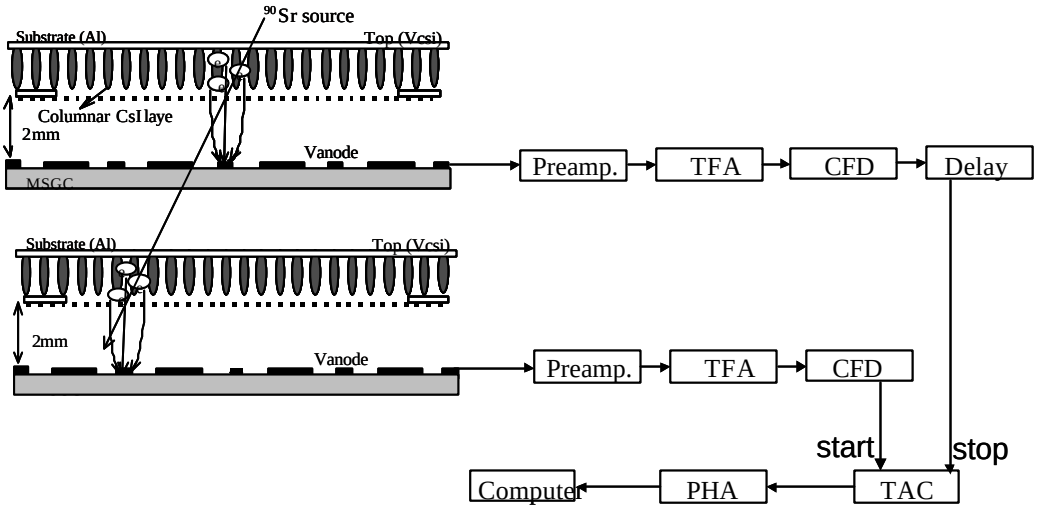

(a)

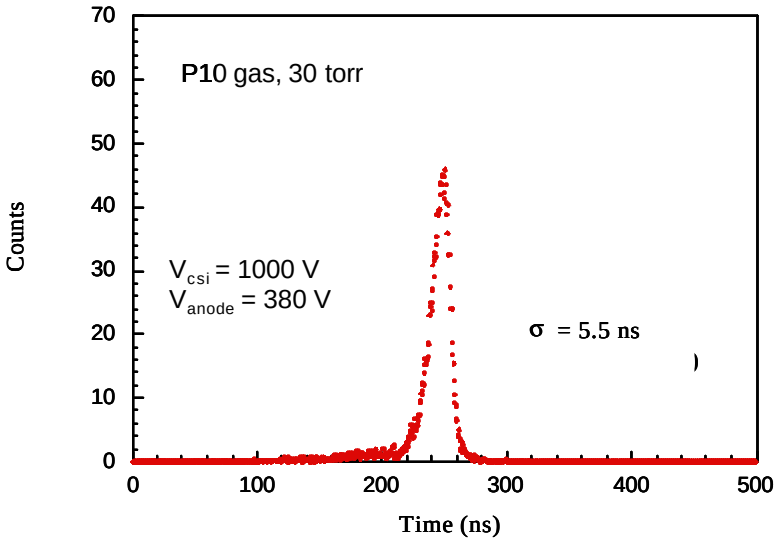

(b)

Figure 4: (a) Timing measurement system of MSGC when a columnar CsI layer was used as a drift plane (b) Timing spectrum at reduced gas pressure, 30 torr.

IV. Electric Field Simulation in a Parallel Plate Geometry

Using the computer program Maxwell [7], we performed a simulation of the electric field for a parallel plane structure consisting of a columnar CsI layer as the cathode plane and a metal-coated glass plate as the anode plane. This geometry is shown schematically in Figure 5.

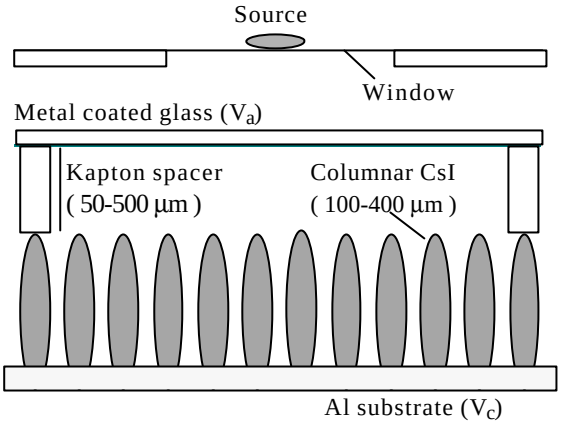

Figure 5: A schematic of a columnar CsI layer and metallic anode. V_a is a voltage on the metallic anode, and V_c is a voltage on the CsI cathode layer.

The simulation was performed for a columnar CsI layer of 100 μm thickness, with a 125 μm gas gap between the top of the CsI and the anode. CsI has a resistivity of 10^{11} Ωcm, which is essentially small relative to that of the gas media. Therefore, we can assume that the columnar CsI layer has everywhere the same potential. Using this model, we determined the map of the electric field lines, which is shown in Figure 6.

Field simulation using the 2D Maxwell program provides an qualitative understanding of the columnar CsI operation. A map of the field lines, and the field strength near the top of the CsI layer are shown in Figure 6(a) and Figure 6(b). In Figure 6(b), the relative field strength for the field strength at the surface of the anode plane is plotted along a trajectory lying 1 μm above the top of the columnar CsI layer. The corresponding field strength at the surface of the anode plane is 6×10^6 V/m.

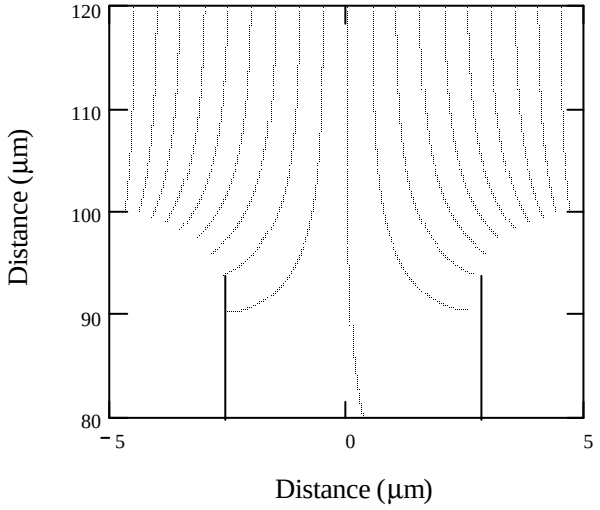

(a)

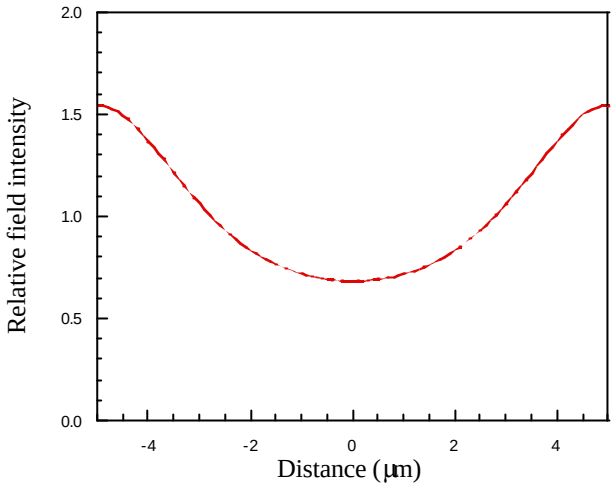

(b)

Figure 6: (a) Maxwell simulation of the electric field, for 100 μm thickness columnar CsI layer with a 125 μm gas gap indicated (b) Calculated field strengths along the dashed line, 1μm above the top of the CsI layer. The relative field strength is defined as a ratio of the field strength at the indicated point for the uniform field strength at the surface of the anode plane. The applied voltage on the anode electrode was 0 V, and on the Al substrate of columnar CsI was 800 V.

The field strength on the tip of the columns is about 1.5 times higher than uniform value of field near the anode. Therefore, in the presence of an incident charged particle, the gas avalanche is most intense near the top of CsI layer. However, the gap between the columns does not have enough field for gas avalanching to occur there, the field strength is much too small even to drift electrons out from between columns of the CsI layer: the field intensity decreases rapidly in the gap between the CsI columns. The result is that only the secondary electrons ejected from near the tip of columnar layer can contribute to the signal.

It is predicted by this simulation that the efficiency of the columnar CsI layer is much smaller than we expected, due to lack of contribution of secondary electron coming from the columnar walls. To verify this simulation, we measured the efficiency of a columnar CsI layer for different thicknesses.

V. Secondary electron efficiency measurements of the columnar CsI layers.

Figure 7 shows the experimental system used for efficiency measurements. Beta rays from a ^{90}Sr source. were directed onto the CsI layer. A MSGC was used as a trigger to count only the high energy (> 1 MeV) tail of the beta spectrum. The efficiency was defined as :

$$Efficiency = \frac{Count\ rate of\ coincidence}{Count\ rate of\ bottom\ MSGC}$$

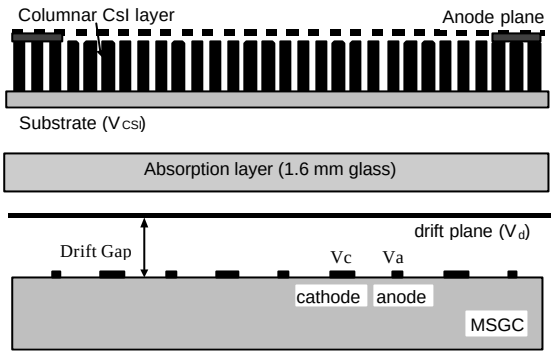

Figure 7: Coincidence measurement system of detection efficiency of a columnar CsI layer. A MSGC was used for a beta-ray trigger. The drift gap was 1.5 mm and the distance between MSGC anode and cathode was 200 μm. V_d = 1000 V, V_a = 460 V and V_c = 0 V. A negative voltage, V_{csi}, was applied to the CsI substrate, and the anode voltage of the columnar CsI was kept at 0 V.

P10 gas was used for the measurement. The electrons produced in the columnar CsI detector arise from two different mechanisms. One source is gas ionization due to the beta-ray in the gap between the anode and CsI layer, and the other is the production of secondary electrons from the CsI surface by bombardment of the beta-rays. Figure 8(a) shows the resulting pulse height spectra from the CsI detectors. The pulse height analyzer (PHA) channel numbers are calibrated in number of collected electrons. The collected average electron numbers as a function of applied voltage for 100 μm and 400 μm thickness CsI layers are shown in Figure 8(b), which the gas gap was 250 μm. The maximum collected electron number before the breakdown was about 6×10^5 for either CsI.

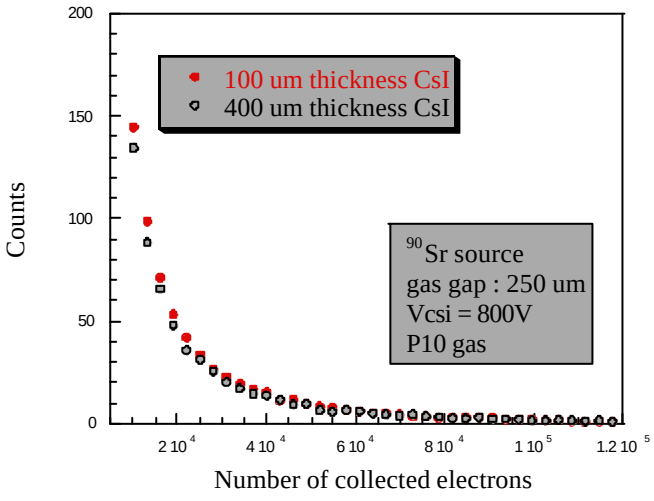

(a)

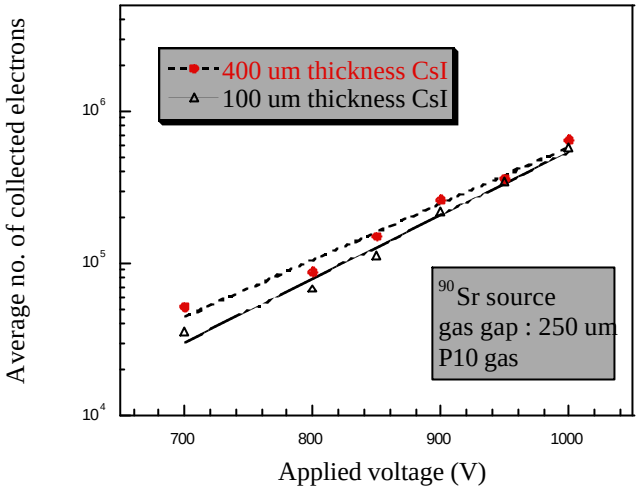

(b)

Figure 8: (a) Pulse height spectra from 100 μm and 400 μm CsI layers, using ^{90}Sr source. (b) Average number of collected electrons from the columnar CsI for two different layer thickness, as a function of applied voltage.

The detection efficiency for 100 μm and 400 μm thickness of columnar CsI layers as a function of gas gap is presented in Figure 9. The beta particles enter the detector with 5° dip angle. The efficiency values were measured in the plateau region found by varying V_{csi}.

One can see that there is little difference between the results for 100 μm and 400 μm CsI thickness, indicating that the signal does not come from within the body of CsI layer. The efficiency increases with the gas gap, and for all except the smallest gap, the direct ionization of the gas becomes dominant. However, a contribution from the CsI secondary electron emission is seen to exist as the gap size is extrapolated to zero. From this result, we estimate that the efficiency of the columnar CsI layer alone to be about 6 % for layers of either thickness.

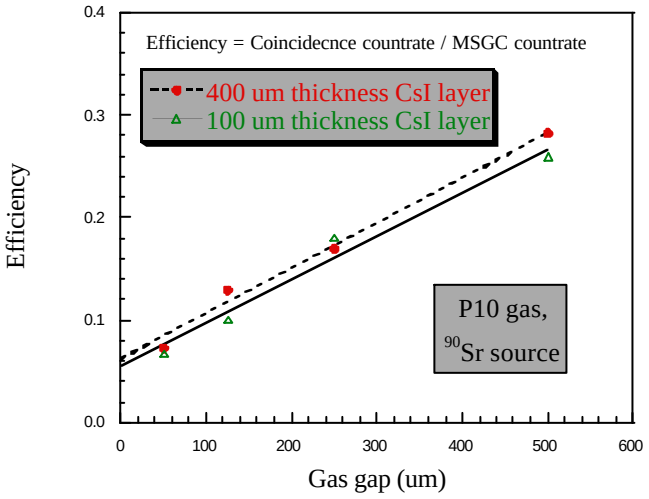

Figure 9: Efficiency for 100 μm and 400 μm thickness of columnar CsI layer as a function of a different gas gap.

This confirms our simulation, which indicates that only the secondary electrons ejected from the end of columns can contribute to the signal, and this explains why the efficiency doesn't depend on the columnar thickness

VI. Discussion

The columnar CsI was initially proposed as an efficient source of ionization for gas avalanche micro-detectors. Since the incident charged particle intercepts many surfaces of the columnar layer, it was hoped that the columnar structure would improve the secondary emission efficiency compared to a single layer. However, we found that the electric field does not penetrate into the space between CsI columns sufficiently to produce avalanches or to extract the secondary electrons. Therefore, only the secondary electrons produced near the top of columnar layer can be detected, and our initial goal with regard to using a columnar CsI layer to provide an efficient secondary emission source for detection of charged particles was not achieved. This is due to the low efficiency of the columnar region of the CsI layer. Using a ^{90}Sr source, we measured an secondary emission efficiency of ~6 % for the columnar layers.

In order to design a detector having high efficiency independent of incident angle, we suggest a new technique consisting of arrays of holes in a substrate, with steep wall sides and secondary emitter coatings. We have successfully fabricated hole arrays on a plastic substrate made of polymethylmethacrylate (PMMA), using "deep X-ray lithography", which is also referred to as the "LIGA process" [8].

The merit of this process is that a high aspect ratio (ratio of the substrate thickness to hole diameter), can easily be achieved, up to ratios of about 200. However, a more important property is that a conducting coating can be placed upon the top and bottom surfaces, allowing a strong electric field to be created within the holes, strong enough to produce avalanches in the holes. Furthermore, the walls of the holes can be coated with a secondary emitter, enhancing the performance. Figure 10 shows an example of this basic structure. Another group has successfully tested a capillary plate with a similar geometry, but using lead glass, and for a different application [9]. Gas avalanche gains of 10,000 were obtained, demonstrating that this approach is sound.

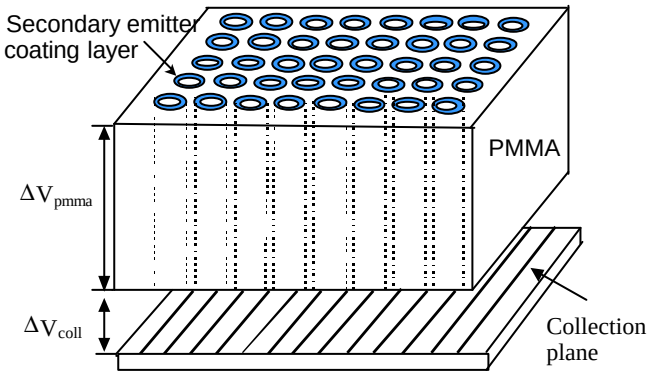

Figure 10: Schematic structure of the secondary emission gas avalanche detector with two gas avalanche regions, ΔV_{pmma} is a voltage across between the PMMA top and bottom. ΔV_{coll} is a

voltage across between the bottom of PMMA and the collection electrode. The walls of the holes are, in general, coated with a secondary electron emitter (e. g. CsI).

Secondary electron emission from the walls of the holes and direct gas ionization in the holes will initiate gas avalanches, and the resulting electrons will be transported out of the holes and detected. Estimates based upon simulations using the GARFIELD program and direct calculations predict that, even for large dip angles as large as 30°, efficiencies of nearly 100% will be obtained, and space resolutions will be much superior to those obtained in a typical MSGC for the same incident angle. The latter improvement results from the much more compact source of primary electrons (a factor of five in the example below).

As an example, we investigate the design involving PMMA layer 600 μm thick (0.17 % radiation length), a hole size of 30 μm, and a pitch of 35 μm. If we consider a 30° dip angle of the incident particle, then the number of holes crossed is nearly 10 , and the number of wall surfaces intercepted is nearly 20 in this structure. We have made the following estimate of the detection efficiency under this condition.

At such an oblique angle to the hole walls, we expect a secondary electron emission efficiency greater than that which we measured as 6 % (in agreement with other results) at normal incidence, but we will use 6 % per surface as a conservative estimate for the purpose of this example. In addition, gas ionization in the hole contributes about 18 % per hole at this dip angle. For the ~30 % per hole probability of obtaining an electron, on average, and assuming each lead to detectable avalanches, the mean number of holes with detectable signals is 3.0, and the overall detection efficiency is 95 %.

The measure of improvement over a typical MSGC spatial resolution may be gauged by the ratio of sensitive gaps, ~3.0 mm for the MSGC, and only 0.6 mm for the present design, a factor of five improvement. We expect the 300 μm resolution measured for an MSGC with $\theta_{dip} = 30^0$, to be greatly improved with the present technique.

Figure 11 shows a simulation of a gas avalanche using the GARFIELD program [10]. For the simulation, an applied voltage across the PMMA produced an electric field within the hole sufficient to produce an avalanche, and an additional field was provided for a "collection region". A detector could be placed after this collection region, or the detection should be done by collection electrodes (strips or pads) placed directly at the exit of the LIGA holes.

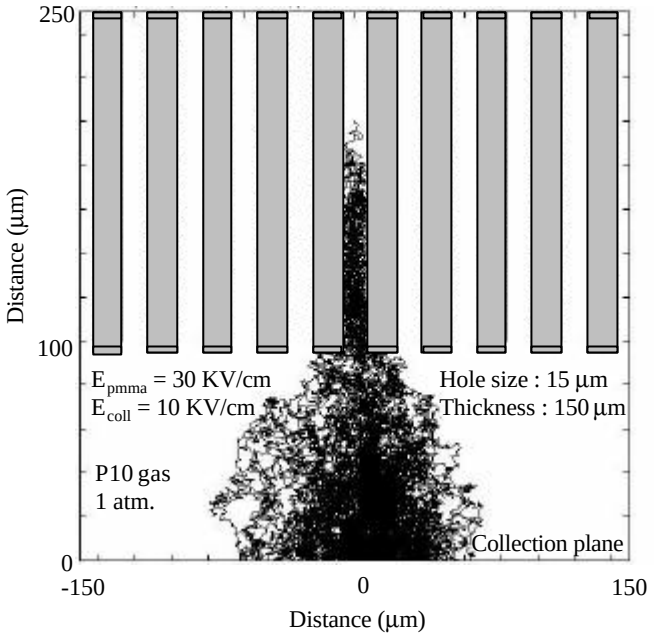

Figure 11: A simulation of a gas avalanche using the GARFIELD program for a PMMA layer coated with secondary emission material.

In the simulations, it was found that fields at least as large as 30 KV/cm were required within the holes to sustain avalanches using P10 gas. However, PMMA is capable of sustaining fields much larger than this, and results are presented at this conference showing gains higher than 3,000 as measured by our group using LIGA micro-hole arrays, having 150 μm hole diameter and 350 μm thickness PMMA, fabricated at LBNL [8].

These simulations and measurements show good prospects for development of this type of gas avalanche micro-detector, permitting a design without a drift region, and with very good detection efficiency, space resolution, and timing characteristics. The results obtained thus far will be the basis for further study.

VI. Reference

[1] H.S. Cho, I.J. Park, W.S. Hong, V. Perez-Mendez and J. Kadyk, "Utilization of a thin columnar cesium iodide (CsI) layer in gas avalanche microdetector," Nucl. Instr. and Meth., A422, pp.269-272, 1999.

[2] I. Frumkin, A. Breskin, R. Chechick, V. Elkind and A. Notea, "Properties of CsI-based gaseous secondary emission x-ray imaging detectors," Nucl. Instr. and Meth., A329, pp.337-347, 1993.

[3] D.F. Anderson, S. Kwan and M. Salomon, "A low-pressure, micro-strip gas chamber operated with secondary-electron emission," Nucl. Instr. and Meth., A348, pp.102-106, 1994.

[4] A. Akkerman, A. Gibrekhterman, A. Breskin, R. Chechick, "Monte Carlo simulations of secondary electron emission from CsI, induced by 1-10 keV x-rays and electrons," J. Appl. Phys., 72, pp.5429-5436, 1992.

[5] C. Chianelli, P. Ageron, J.P. Bouvet, M. Karolak, S. Martin and J.P. Robert, "Weakly ionizing charged particle detectors with high efficiency using transitory electronic secondary emission of porous CsI," Nucl. Instr. and Meth., A273, pp245-256, 1988.

[6] T. Jing, C.A. Goodman, J. Drewery, G. Cho, W.S. Hong, H. Lee, S.N. Kaplan, V. Perez-Mendez and D. Wildermuth, "Detection of charged particles and x-rays by scintillator layers coupled to amorphous silicon photodiode arrays," Nucl. Instr. and Meth., A368, pp.757-764, 1996.
[7] MAXWELL Electric Field Simulator, Ansoft Corporation, Pittsburgh, PA 15219, USA.
[8] H.K. Kim, K. Jackson, W.S. Hong, I.J. Park, S.H. Han, J. Kadyk, V. Perez-Mendez, W. Wenzel and G. Cho. "Application of the LIGA process for fabrication of gas avalanche device," Presented at IEEE Nucl. Sci. Symposium, N20-5, Seattle, Oct., 1999.
[9] H. Sakurai, T. Tamura, S. Gunji and M. Noma, "A new type of proportional counter using a capillary plate," Nucl. Instr. and Meth., A374, pp.341-344, 1996.
[10] GARFIELD, Version 8, CERN